Maghrebian Journal of Pure and Applied Science

ISSN : 2458-715X

http://revues.imist.ma/?journal=mjpas&page=index

Inhibition Effect of 6-bromo-3-nitro-2-phenylimidazol [1,2-α] pyridine on the Corrosion of C38 Steel in H_2SO_4 Solution.

A. Anejjar[1], R. Salghi[1,*], S. Jodeh[2], Y. Karzazi[3], I. Warad [2], R. Dassanayake [4], O. Hamed[2], A. Zarouk[4], B. Hammouti[4]

[1] *Laboratory of Applied Chemistry and Environment, ENSA, Université Ibn Zohr,PO Box 1136, 80000 Agadir, Morocco*

[2] *Department of Chemistry, An-Najah National University, P. O. Box 7, Nablus, Palestine.*

[3] *National School of Engineering and Applied Sciences, University Mohammed Premier,P. O. Box 3, 32003 SidiBouafif, ENSA Al Hoceima, Morocco.*

[4]*Fiber & Biopolymer Research Institute, Texas Tech University, Lubbock, TX 79403, USA.*

[5]*Laboratory of Applied Chemistry and Environment (URAC 18), Faculty of Sciences,University Mohammed Premier, P. O. Box 4808, 60046 Oujda, Morocco*

[*]*E-mail: Prof. R. SALGHI, Phone: 00212661145512, Email: r.salghi@uiz.ac.ma,*

Abstract

The inhibition effect of 6-bromo-3-nitro-2-phenylimidazol[1,2-α] pyridine (**BNPP**) on the corrosion of C38 steelin 0.5 M H_2SO_4 was studied by weight loss , electrochemical methods. The results showed that **BNPP** was a good inhibitor in 0.5 M H_2SO_4 and this adsorption obeyed the Langmuir adsorption isotherm. The results obtained from the different corrosion evaluation techniques are in good agreement. Polarization curves showed that **BNPP** acted as a mixed-type inhibitor in sulfuric acid. The effect of the temperature on the corrosion behavior with addition of 10^{-3}M of the inhibitor was studied in the temperature range 298-328 K, and the thermodynamic parameters were determined and discussed. Quantum chemical approach, using the density functional theory (DFT), was applied in order to get better understanding about the relationship between the inhibition efficiency and molecular structure of BNPP. The theoretical results were found to be consistent with the experimental data.

***Keywords*:** C38 Steel, EIS, Polarization, Weight loss, Acid inhibition

1. INTRODUCTION

Acid solutions are generally used for the removal of undesirable scale and rust in several industrial processes. Inhibitors are used in these processes to control metal dissolution as well as acid consumption.The uses of inhibitors are one of the most practical methods to inhibit corrosion of metals in many environments, especially in acidic media [1].The role of inhibitors added in low concentrations to corrosive media is to decrease the dissolution of the metal with corrosive medium and is to inhibit the adsorption or coordination onto the metal surfaces [2,3].Organic compounds bearing heteroatoms such as phosphorous, sulfur, nitrogen, oxygen or those containing multiple bonds which are considered as adsorption centers, are effective as the corrosion inhibitor [4,14]. Up to now, various N-heterocyclic compounds are described as good corrosion inhibitors for steel in acidic media, such as pyrazoles [15-18], triazoles [19- 22], tetrazoles [23-26], imidazole derivatives [27-31], pyridine [32-36] and imidazopyridine [37-44]. These compounds can adsorb onto the steel surface and block active sites, thus decreasing the corrosion rate[45,46].According to our recent work [41], the imidazopyridine derivatives newly synthesized named 6-bromo-3-nitro-2-phenylimidazol[1,2-α] pyridine**(BNPP,** Fig. 1**)** act as good corrosion inhibitors on the corrosion ofC38 steel in 1.0 M HCl. In a continuation of our works, the inhibition effect of**BNPP**on the corrosion of C38 steel in 0.5M H_2SO_4 solution was studied using weight loss, potentiodynamic polarization curves and electrochemical impedance spectroscopy (EIS) methods. The adsorption isotherm of inhibitor on steel surface and the standard adsorption free energy (ΔG_{ads}) are obtained. The effect of temperature is studied and the thermodynamic parameters are also calculated and discussed in detail.

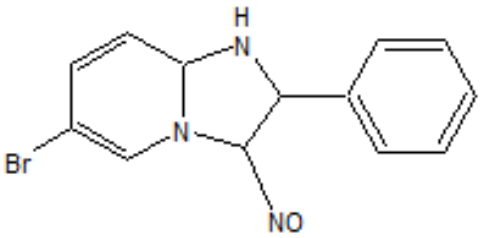

Fig. 1. The molecular structures of **BNPP**

2. EXPERIMENTAL

2.1. Materials

The steel used in this study was a C38 steel (Euronorm: C35E carbon steel and US specification: SAE 1035) of chemical composition (wt%) of 0.370 % C, 0.230 % Si, 0.680 % Mn, 0.016 % S, 0.077 % Cr, 0.011 % Ti, 0.059 % Ni, 0.009 % Co, 0.160 % Cu, and the remainder iron (Fe). Before the experiments the C38 steel samples were pre-treated by grinding with emery paper SiC (320, 800, and 1200 grade), rinsing with distilled water, degreasing by immersion in acetone in an

ultrasonic bath for 5 min, washing again with bidistilled water, and then drying at room temperature. The acid solutions (0.5 M H_2SO_4) were prepared by dilution of analytical reagent-grade 98 % H_2SO_4 with double-distilled water. The range of concentration of **BNPP** was 10^{-6} M to 10^{-3} M.

2.2. Weight loss measurements

Gravimetric measurements were performed after 6 h at room temperature, by use of an analytical balance (precision ± 0.1 mg). The C38 steel specimens used were rectangular in shape (length = 1.6 cm, width = 1.6 cm, thickness = 0.07 cm), and treated as cited above. The temperature was controlled at 298 using a water thermostat. Gravimetric experiments were performed in a double glass cell equipped with a thermostated cooling condenser containing 80 mL non-de-aerated test solution. After immersion, the C38 steel specimens were withdrawn, carefully rinsed with bidistilled water, cleaning ultrasonically in acetone, dried at room temperature, and then weighed. Triplicate experiments were performed in each case and the mean value of the weight loss was calculated.

2.3. Electrochemical measurements

Electrochemical experiments were conducted by use of impedance equipment (Galvanostat/Potentiostat PGZ 100) controlled with TacusselVoltaMaster 4 corrosion analysis software. A conventional three-electrode cylindrical Pyrex glass cell was used. The temperature was thermostatically controlled. The working electrode was C38 steel with the surface area of 1 cm^2.Asaturated calomel electrode (SCE) was used as reference. The counter electrode was a platinum plate of surface area 1 cm^2. For polarization curves, the working electrode was immersed in test solution for 30 min or until a steady-state open circuit potential (E_{ocp}) was obtained. The polarization curve was recorded by polarization from -750 to -200 mV/SCE with a scan rate of $1mV.s^{-1}$. AC impedance measurements were performed in the frequency range 100 kHz–10 mHz, with 10 points per decade, at the rest potential, after immersion in acid for 30 min, by applying 10 mV ac voltage peak-to-peak. Nyquist plots were obtained from these experiments. To produce the Nyquist plot, the data points were fitted to the best semicircle, by use of a non-linear least square fit, to give the intersections with the x-axis.

2.4. Quantum Chemical Calculations

Full geometry optimization with no constraints of **BN**PP was performed using DFT based on Beck's three parameter exchange functional and Lee–Yang–Parr nonlocal correlation functional (B3LYP) [67-

69] and the 6-31g(d,p) orbital basis sets for all atoms as implemented in Gaussian 09 program [70]. The calculated molecular properties include the highest occupied molecular orbital (HOMO), lowest unoccupied molecular orbital (LUMO) and other molecular properties derived from HOMO and LUMO and their respective energies. Molecular modeling study was carried out to determine the electron rich groups/atoms in a molecule as well as calculation of the HOMO and LUMO in order to give further insights on the possibility of electron transfer between the inhibitor and metal.

2.5. Optical microscopy

Immersion corrosion analysis of C38 samples in the acidic solutions with and without the optimal concentration of the inhibitor was performed using optical microscopy (OM). Immediately after the corrosion tests, the samples were subjected to OM studies to examine the surface morphology. The working sample was analyzed at three different locations to ensure reproducibility.

3. RESULTS AND DISCUSSION

3.1 Weight loss measurements

The corrosion rate (W_{corr}) of tested metal in 0.5 M H_2SO_4 solution at different concentrations of BNPP was determined after 6 h of immersion time at 298 K and calculated using the following equation:

$$W_{corr} = \frac{m}{S.t} \qquad (1)$$

where m is the weight loss of C38 steel sheets, S the total area of C38 steel sheets and t is immersion time.

The obtained values of the gravimetric corrosion rates (W_{corr}) and the inhibition efficiency (E_w) are represented in Table 1.

Table 1. Corrosion data obtained from measurement of weight loss of C38 steel in 0.5 M H_2SO_4 containing different concentrations of **BNPP** at 298 K.

Inhibitor	Conc. (M)	Conc. (M)	E_w(%)
Blank	0	1.5482	-
NBPP	10^{-3}	0.2146	86.14
	10^{-4}	0.2481	83.97
	10^{-5}	0.2742	82.28
	10^{-6}	0.3328	78.50

The inhibition efficiency (E_w) (%) corrosion in the case of this method was calculated from the following equation:

$$E_w(\%) = \frac{W_{corr} - W'_{corr}}{W_{corr}} \times 100 \qquad (2)$$

where $W_{corr}$and $W'_{corr}$are the corrosion rates of C38 steel due to the dissolution in 0.5 M H_2SO_4 in the absence and the presence of definite concentrations of **BNPP**, respectively.

The results obtained from gravimetric measurements show for inhibitor tested that the corrosion rate values decrease when the concentration of **BNPP** increases. The analysis of table 1show that protection efficiency increased with the increase in concentration from 10^{-6}M to 10^{-3}M for the inhibitor studied. We noted that **BNPP** used in this study showed excellent corrosion inhibitor for C38 steel in 0.5 M H_2SO_4, especially forlowconcentration (78.50 % for 10^{-6}). The best action is attained in the presence of 10^{-3}M of **BNPP**.

It should be noted that organic compounds are known to yield unreliable and irreproducible results for concentrations higher than 2 x 10^{-2}M [47-49]. For this reason, in this present test concentrations were up to 10^{-3} M only. Inhibition of corrosion of C38 steel by **BNPP** can be explained on the basis of adsorption on the metal surface. This compound can be adsorbed on the metal surface by interaction between the metal surface and lone pairs of electrons of nitrogen and oxygen atoms and the π-electrons of the heterocyclic structure of the inhibitor [50]. This process is facilitated by the presence of vacant orbitals of low energy in iron atoms, as observed for other transition group metals [51, 52].

3.2. Electrochemical impedance spectroscopy (EIS).

Fig. 2represent the Nyquist diagram for C38 steel in 0.5 MH_2SO_4in the absence and the presence at different concentrations of **BNPP** plotted at open circuit potential (E_{corr}) at 298 K after 30 min.

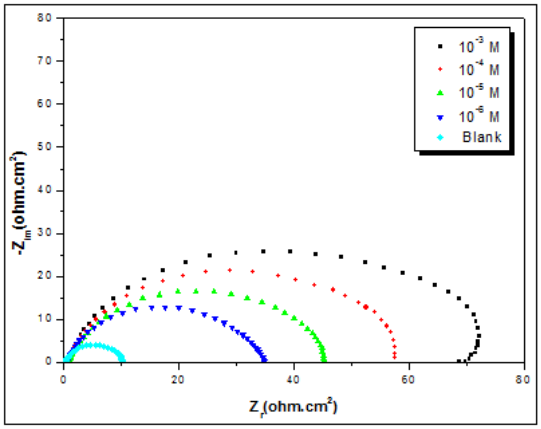

Fig. 2. Nyquist plots of the corrosion of C38 steel in 0.5 M H_2SO_4 without and with different concentrations of **BNPP** at 298K.

The impedance parameters of C38 steel in 0.5M H_2SO_4 containing different concentrations of BNPP is show in the Table 2.

The impedance spectra show a large capacitive loop at high frequencies followed by a small inductive loop at low frequency values. In the presence of inhibitor, comparing with blank solution, the shape is maintained throughout all tested concentrations, indicating that almost no change in the corrosion mechanism occurs due to the inhibitor addition [53, 54]. The capacitive loop at high frequency indicates that the corrosion of C38 steel is mainly controlled by a charge transfer process, as is usual in EIS studies, the high frequencies capacitive loop is related to the charge-transfer process occurring during metal corrosion and the double-layer behavior [55].

While the inductive loop at low region frequency is relates to the relaxation process of the adsorbed intermediates controlling the anodic process [56] or inhibitor species on the electrode surface [57].

The diameters of capacitive loops increase with the increase in **BNPP** concentration, which indicates the increase of charge transfer resistance and improvement in inhibiting effect on C38 steel corrosion (Fig. 2). It is also observed that the shapes of the impedance plots for the inhibited electrodes are not essentially different from those of the uninhibited electrodes.It reveals that the presence of **BNPP** in 0.5 M H_2SO_4solutions increases the charge transfer impedance due to the formation of protection layer on the C38 steel surface, but it does not change other aspects of the corrosion behavior.

Table 2. Impedance parameters of C38 steel in 0.5M H_2SO_4 containing different concentrations of imidazopyridine**BNPP**.

Inhibitor	Conc. (M)	R_{ct} ($\Omega.cm^2$)	f_{maxc} (Hz)	C_{dl} ($\mu F/cm^2$)	E_{Rtc} (%)
Blank	0	10	158	100.78	----
NBPP	10^{-3}	70	63	36.11	85.71
	10^{-4}	57	75	37.25	82.46
	10^{-5}	45	80	44.23	77.78
	10^{-6}	35	100	45.49	71.43

The charge-transfer resistance values (R_{ct}) were calculated from the difference in real impedance at lower and higher frequencies as suggested by Tsuru et al. [58]. To obtain the double-layer capacitance (C_{dl}), the frequency at which the imaginary component of the impedance is maximum($-Z_{max}$) is found and C_{dl} values were obtained from the Eq. (3):

$$f(-Z\max) = \frac{1}{2.\pi.C_{dl}.R_{ct}} \qquad (3)$$

with C_{dl}: Double layer capacitance ($\mu F.cm^{-2}$); f_{max}: maximum frequency (Hz) and R_{ct}: Charge transfer resistance ($\Omega.Cm^{-2}$).

The inhibition efficiency is calculated using charge-transfer resistancefrom Eq. (4):

$$E_{Rct}(\%) = \frac{(R_{ct} - R^{\circ}_{ct})}{R_{ct}} x100 \qquad (4)$$

Were R_{ct} and R^0_{ct} are the charge transfer resistances in inhibited and uninhibited solutions respectively.Results obtained show that R_{ct} increases and C_{dl} tends to decrease with increasing of inhibitor concentration.The decrease in C_{dl} in comparing with that in blank solution, which can result from a decrease in local dielectric constant and/or an increase in the thickness of the electrical double layer, suggests that the inhibitor molecules function by adsorption at the metal/solution interface [59, 60]. These results again confirm that **BNPP**exhibit good inhibitive performance for C38 steel in H_2SO_4 solution.

3.3. Potentiodynamic polarization curves

To confirm the above results and to study the inhibition mechanism in more detail, potentiodynamic polarization technique was used. The polarization curves of C38 steel in 0.5 M sulfuric acid solutions obtained with and without various concentrations of used inhibitor are shown in Fig.3.

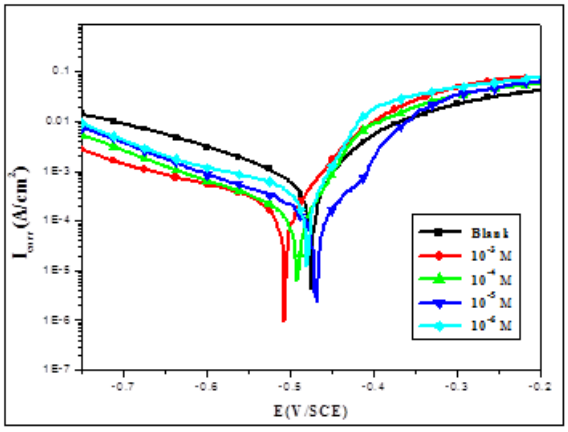

Fig. 3. Polarization curves of C38 steel in 0.5 M H_2SO_4 containing different concentrations of **BNPP**

The corrosion current density (I_{corr})values were used to calculate the inhibition efficiency, E_I (%), by use of the equation:

$$E_I\% = \frac{(I^o_{corr} - I_{corr})}{I^o_{corr}} x\,100 \qquad (5)$$

where I^o_{corr} and $I_{corr}$are the corrosion current densities for C38 steel electrode in the uninhibited and inhibited solutionsrespectively, determined by extrapolation of cathodic Tafel lines to the corrosion potential.

The electrochemical corrosion parameters including corrosion current densities (I_{corr}), corrosion potential (E_{corr}), cathodic Tafel slope (b_c) and corresponding inhibition efficiency E_I (%) are given in Table 3.

Table 3. Polarization data of C38 steel in 0.5 M H_2SO_4 without and with addition of inhibitor at 298 K.

Inhibitor	Conc. (M)	E_{corr} (mV/SCE)	I_{corr} (µA/cm^2)	-b_c (mV/dec)	E (%)
Blank	0	478	1860	189	----
BNPP	10^{-3}	506	250	149	86.56
	10^{-4}	493	280	158	84.95
	10^{-5}	468	320	171	82.79
	10^{-6}	481	378	164	79.68

Inspection of polarization curves and electrochemical parameter (Table.3) reveals that cathodic current densities decrease with the increase of the inhibitor concentration and the inhibition effeciencyE_I(%)

increases with the inhibitor concentration up to a maximumof 86.56%, due to the increase in the blocked fraction of the electrode surface by adsorption.

The anodic curves of C38 steel in 0.5 M H_2SO_4 in the presence of **BNPP** show that the additionof the inhibitor concentration decreases also the anodic current densities. The presence of **BNPP** displaces E_{corr} towards more negative potentials; this displacement in E_{corr} is < 85 mV. This result shows that **BNPP** influences both cathodic and anodic branches.This implies that the inhibitor, **BNPP**, acts as a mixed-type inhibitor, affecting both anodic and cathodic reactions[61]. According to Riggs and coworkers [62], if the displacement in corrosion potential is more than ±85 mV/SCE with respect to the corrosion potential of the blank, the inhibitor can be classified as a cathodic or anodic type, but the maximum displacement in the present case is less than 30 mV/SCE, which indicates that **BNPP** is a mixed-type inhibitor; as reported in our resent work [40]

As would beexpected both anodic and cathodic reactions of C38 steel corrosion in sulphuric acid solution were reducted, and this inhibition effect became more important with increasing **BNPP** concentration.This result suggests that the addition of the inhibitor reduces the anodic oxidation of C38 steel and also retards the hydrogen reduction reaction.This reduction of the corrosion process can be attributed to the covering of adsorbed inhibitor molecules on the C38 steel surface. [63]

Inhibition efficiencies obtained from weight loss (E_w), electrochemical impedance spectroscopy and potentiodynamic polarization curves are in good reasonably agreement.

3.4. Effect of temperature.

Temperature can modify the interaction between the C38 steel electrode and the acidic medium in the absence and the presence of inhibitors. To assess the influence of temperature on corrosion and corrosion inhibition processes,polarization tests were carried out at various temperatures (298–328 K) in the absence and presence of 10^{-3}M of **BNPP**, as shown in Fig. 4. Corresponding electrochemical data are given in Table 4.

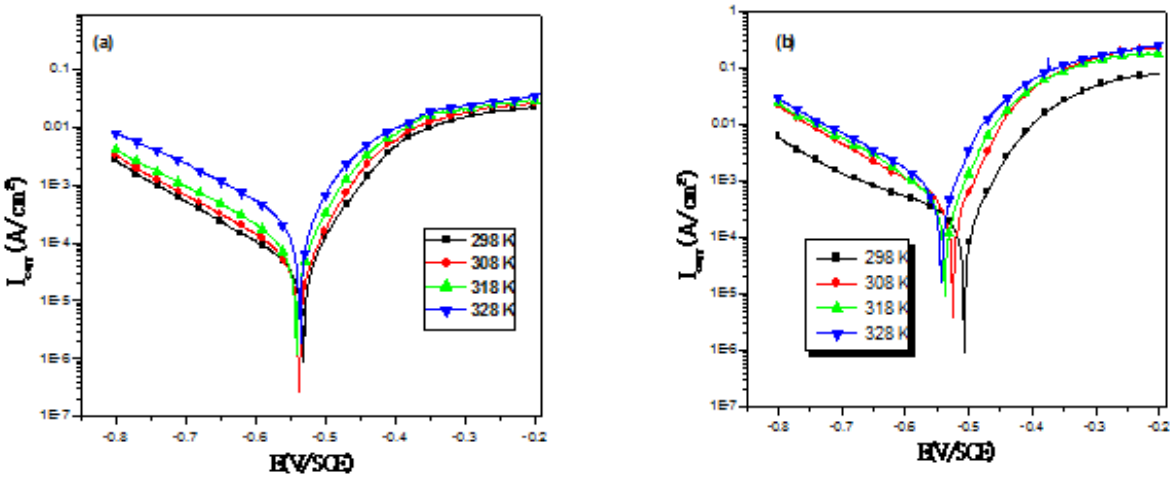

Fig. 4. Polarization curves of C38 steel in 0.5 M H_2SO_4 solution in the absence (a) and presence (b) of 10^{-3} M of **BNPP** at different temperatures after 30 min immersion

Table 4. Electrochemical parameters of the C38 steel in 0.5 M H_2SO_4 solutions in the absence and presence of 10^{-3} M of inhibitor.

Inhibitor	Temp. (K)	E_{corr} (mV/SCE)	I_{corr} ($\mu A/cm^2$)	$-b_c$ (mV/dec)	E (%)
Blank	298	-478	1860	190	----
	308	-483	2754	151	----
	318	-493	3036	126	----
	328	-497	4511	104	----
NBPP	298	-506	250	149	86.56
	308	-525	417	159	84.86
	318	-537	553	141	81.78
	328	-542	895	133	80.16

As seen from Fig.4 (a and b)and Table 4, the corrosion current density increases with increasing temperature, in both uninhibited and inhibited solutions.Inhibition efficiency for **BNPP** decreases with increase in temperature and a slight changes inthere values are observed in the range of temperature studied. Thus the compounds can be regarded as temperature-independent inhibitors.

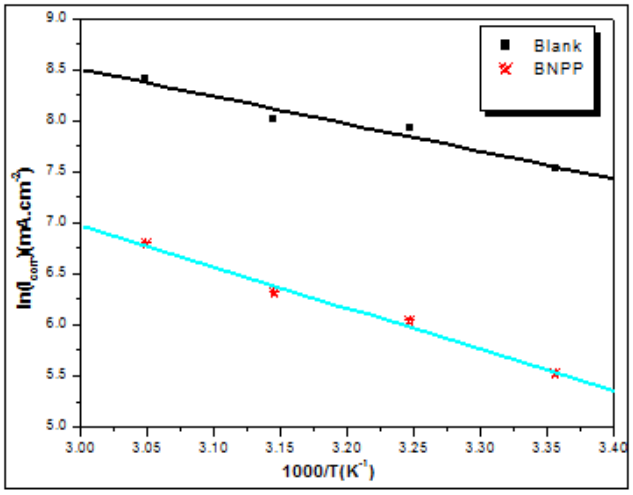

Fig.5. Arrhenius plots of C38 steel in 0.5M H_2SO_4 with and without 10^{-3}M of **BNPP**.

The nearly constant efficiency of the inhibitors in the temperaturerange studied can be considered as the slight change in thenature of the adsorption mode: physisorption of the inhibitor isdominant in the temperature range studied, while chemisorptionaccompanied by physisorption can occur slightly with increasingthe temperature.To calculate the activation parameters of the corrosion process,Arrhenius (eq.6) was used [64].

$$I_{corr} = A\exp(-\frac{E_a}{R.T}) \qquad (6)$$

Where k is the pre-exponential factor, Ea is the apparent activationenergy of the corrosion process, R is the gas constant and T is theabsolute temperature.

Fig. 5 shows Arrhenius plots of the logarithmof the current density vs 1/T for C38 steel in the corrosive mediumwith and without addition of 10^{-3}M of **BNPP**. Straightlines are obtained with a slope of ($-E_a/R$). Activation energy (E_a) values are deduced from this graph and listed inTable 5.

Table 5. The values of activation parameters E_a, ΔH^*, $\Delta S^*$and ΔG^* for C38 steel in 0.5M H_2SO_4 in the absence and the presence of 10^{-3} M of **BNPP**.

Inhibitor	E_a (kJ/mole)	ΔH^* (kJ/mole)	ΔS^* (J/mole^{-1}.k^{-1})	ΔG^* (kJ/mole à T=298K)
Blank	22.37	19.77	-115.71	54.25
BNPP	33.37	30.77	-95.51	59.23

From the same table, it is observed that the values of E_a obtained inpresence of **BNPP** are higher than that obtained inthe inhibitor-free solution.The higher E_a value in the inhibited solution can be correlated with the increased thickness of the double layer, which enhances the activation energy of the corrosion process. [65]

The temperature dependence of the inhibiting effect and the comparison of the values of the apparent activation energy of the corrosion process in the absence and presence of the inhibitor can provide further evidence[66,67]concerning the mechanism of the inhibiting action. The decrease of the inhibitor efficiency with temperature rise, which refers to a higher value of E_a, when compared to that in acid media without inhibitor, is explained as an indication for an electrostatic character of the inhibitor's adsorption. The lower value of E_a in an inhibited solution when compared to an uninhibited one shows that chemisorption bond between the inhibitor and the metal is highly probable [68]. Activation energy, E_a values in the table are higher for inhibited solution than the uninhibited media, indicating a high inhibitive action of the additives by increasing energy barrier for the corrosion process, emphasizing the electrostatic character of the inhibitor's adsorption on the C38 steel surface (physisorption).

Thermodynamic parameters, such as enthalpy and entropy of corrosion process, may be evaluated from the effect of temperature. An alternative formulation of Arrhenius equation is (7) [69]:

$$I_{corr} = \frac{RT}{Nh}.\exp(\frac{\Delta S^*}{R}).\exp(-\frac{\Delta H^*}{RT}) \qquad (7)$$

Where N is the Avogadro's number, h the Plank's constant, R is the perfect gas constant, ΔS^* and $\Delta H^*$the entropy and enthalpy of activation, respectively.

Fig. 6 shows a plot of $\ln(I_{corr}/T)$ against 1/T for **BNPP**.Straight lines are obtained with a slope of ($-\Delta H^*/R$) and an intercept of ($\ln R/Nh + \Delta S^*/R$) from which the values of $\Delta H^*$and ΔS^* are calculated respectively and listed in Table 5.

The positive values of ΔH^* both in the absence and presence organic compound reflect the endothermic nature of the C38 steel dissolution process and it indicates that the dissolution of C38 steel is difficult [70].

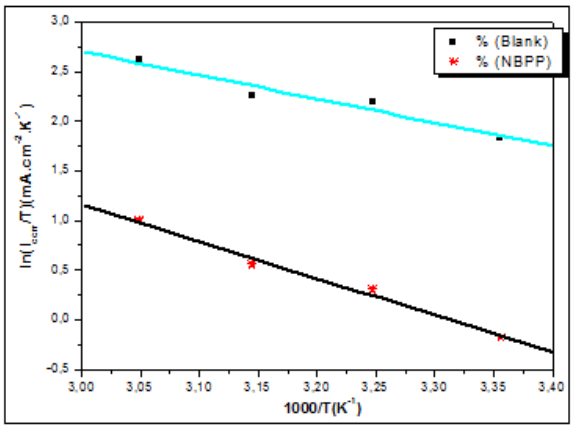

Fig.6. Relation between ln(I_{corr}/T) and 1000/T in sulfuric acid at different temperatures.

From Table 5 , it is clear that entropy of activation ΔS*decreases more negatively in the uninhibited than inhibited systems imply that the activation complex in the rate determining steps represents association rather than dissociation step, meaning that a decrease in disordering takes place on going from reactants to the activated complex[71]. Similar observations have been reported in the literature for mild steel dissolution in the absence and presence of inhibitors in H_2SO_4solution. [68, 72].

3.5. Adsorption isotherm

The type of the adsorption isotherm can provide additional information about the properties of the tested compounds. Attemptswere made to fit experimental data to various isotherms includingFrumkin, Langmuir, Temkin, Freundlich, Bockris-Swinkels, andFlory-Huggins isotherms. By far the results are best fitted by Langmuiradsorption isotherm equation [73]:

$$\frac{C}{\theta} = \frac{1}{K} + C \quad (8)$$

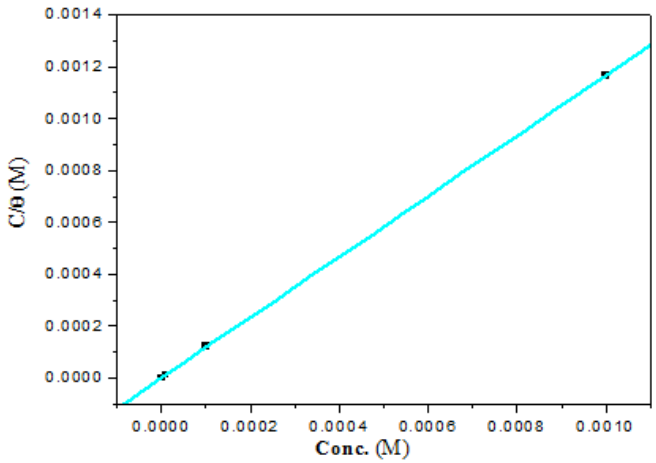

Fig. 7. Langmuir isotherm adsorption mode of **BNPP** on the C38 steel surface in 0.5M H_2SO_4 at 298K from EIS.

Where C is the concentration of inhibitor, K the adsorptive equilibrium constant, and θ is the fraction of the surface covered calculated as follows θ = E(%)/100.

Plots of C/θ against C yield straight lines as shown in Fig. 7, and the corresponding linear regression parameters are listed in Table 6.

Table 6. Parameters of the straight line of C/θ against C and adsorption free energy ΔG_{ads}.

Inhibitor	Slope	$K_{ads}(M^{-1})$	R^2	ΔG_{ads} (kJ/mol)
BNPP	1.16	504894,95	0.99999	-42.47

Both linear correlation coefficient (R) and slope are very close to 1, indicating the adsorption of **BNPP** on C38 steel surface obeys the Langmuir adsorption isotherm in sulfuric acid solutions. The adsorptive equilibrium constant (K) is related to the standard free energy of adsorption (ΔG_{ads}) as shown the following equation [73]:

$$K = \frac{1}{55.5}\exp\left(-\frac{\Delta G_{ads}}{RT}\right) \quad (9)$$

ΔG_{ads} is the standard free energy of adsorption reaction, R is the universal gas constant, T is the absolute temperature (K) and the value of 55.5 is the concentration of water in the solution in mol/L.

The negative values of ΔG_{ads} indicate that the adsorptionof inhibitor molecule on C38 steel surface is spontaneousand also the strong interaction between inhibitor molecules and the metal surface. [74,75-77]

Generally, valuesof ΔG_{ads} up to -20 kJ. mol^{-1} are consistent with the electrostatic interaction between the charged molecules and the charged metal(physical adsorption), the inhibition acts due to the electrostatic interactions between the charged molecules and the charged metal, while the values around -40 kJ/mol or smaller, were seen as chemisorption, which is due to the charge sharing or a transfer from the inhibitor molecules to the metal surface to form a covalent bond [78-79].

In the present work, the value of ΔG_{ads} is found to be around -40kJ.mol^{-1}; means that the adsorption mechanism of **BNPP** on C38 steel surface is mainly the chemisorption.

3.6. Quantum Chemical Calculations

The optimized geometry at the b3lyp/6-31g(d,p) level of **BNPP** and their corresponding frontier molecular orbitals (HOMO and LUMO) are shown in Fig. 8. The energy levels viz., E_{HOMO}, E_{LUMO} and ΔE calculated in atomic units (u.a. or Hartree) are depicted in Table 7.

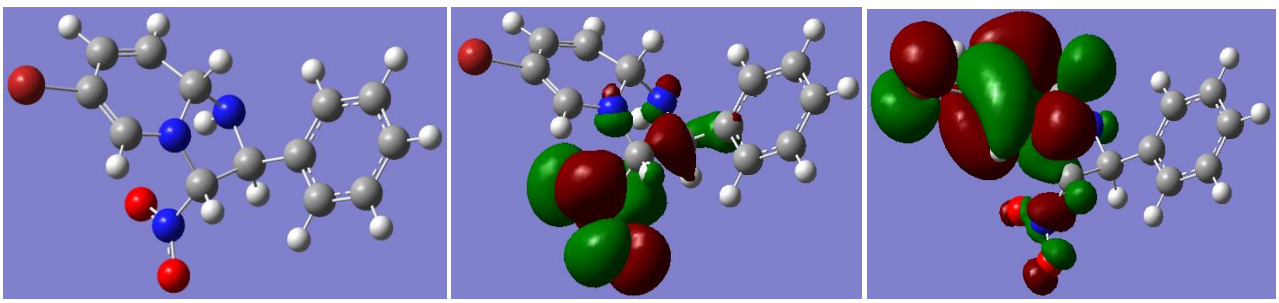

Fig. 8 : Optimized structure, LUMO and HOMO of **BNPP**.

Table 7. Calculated quantum chemical parameters for **BNPP** and iron (Fe, Fe^{2+} and Fe^{3+}).

Compound	E_{HOMO} (a.u.)	E_{LUMO} (a.u.)	$\Delta E=E_{LUMO}-E_{HOMO}$ (a.u.)
BNPP	-0.20350	-0.07275	0.13075
Fe	-0.20181	-0.12376	0.07805
Fe^{2+}	-1.00063	-0.70608	0.29455
Fe^{3+}	-1.76592	-1.12498	0.64094

The HOMO and the LUMO are interesting to investigate because they provide an idea about the regions of the molecule with the tendency to donate or accept electrons. From figure 8, the HOMO is strongly localized on bromine atom, pyridine ring, imidazole and nitro group while the LUMO densities are mainly localized on imidazole and nitro group.

The calculated Mulliken charges on the atoms provide information on the reactivity sites. The highest negative charge is found on the nitrogen atom (-NH-) of the imidazole (-0.503) indicating that this is the atom on which the electrophilic attack would preferably occur.

An ideal corrosion inhibitor has a greater tendency to donate electrons, receive electrons or bind strongly to the metal surface [84] which suggests that **BNPP** may donate electrons to the metal surface through HOMO and accept electrons from the metal surface through LUMO. Further, E_{HOMO} value for **BNPP** was found to be -0.20350 a.u., which was higher (less negative) than that of iron value (-0.20181). The literature shows that E_{HOMO} is often associated with the electron donating ability of the molecule and the inhibition efficiency increases with increase in the values of E_{HOMO}. A higher value of E_{HOMO} for **BNPP** than of iron clearly suggests that it has a greater potential to donate electrons [85].

From Table 7, it is clear that the energy gap values follow the order, Fe <**BNPP**< Fe^{2+}< Fe^{3+}; which suggested that **BNPP** has an ability to donate electrons preferably to Fe^{3+} and Fe^{2+}. Thus, molecular modeling studies supported well the corrosion inhibition potential of **BNPP** while its possible mode of interaction with metal surface.

3.7. Morphological investigation

Surface morphology of C38 steel in 0.5 M H_2SO_4 in absence and presence of **BNPP** inhibitor concentration at 298K were performed and illustrated in Fig.9.

It is clear that the C38 surface was strongly damaged in the absence of inhibitor at 298K temperature (Fig. 9a) compared to the Fig. 9b represent the micrograph obtained of polished steel without being exposed to the corrosive medium, that's due to metal dissolution in corrosive solution, while the surface active of carbon steel was considerably reduced and the smooth surfaces appear by formation of a protective film on the metal surface, the film formed becomes more protective with increase in inhibitor concentration 10^{-3}M at 298K (Fig.9c). This is attributed to the involvement of **BNPP** compound in the interaction with the active sites of metal surface. This results confirmed higher inhibition efficiency of **BNPP**.

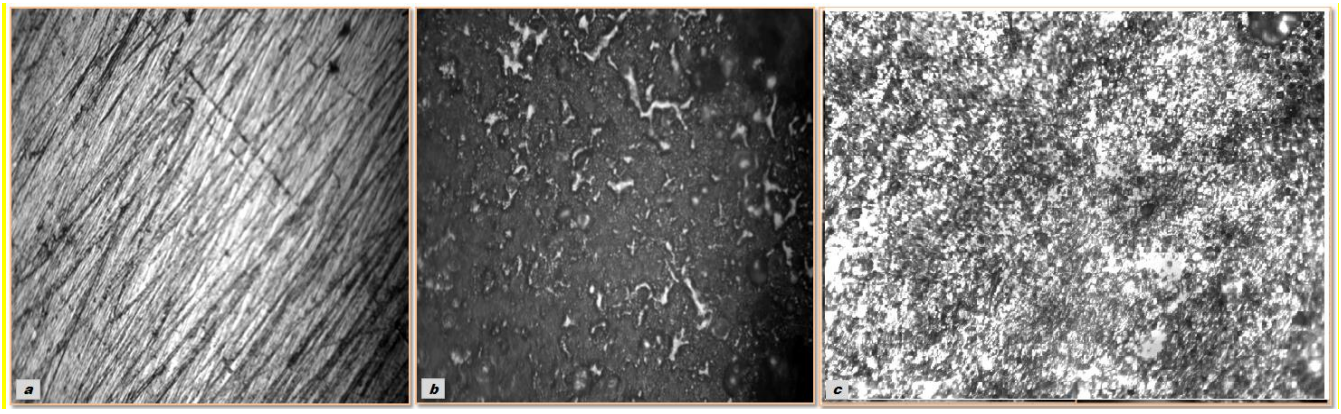

Fig. 9: OM (x200) of tinplate (a) before immersion (b) after 6 hours of immersion in 0.5M H_2SO_4 (C) after 6 hours of immersion in 0.5M H2SO4 + 10-3 M of BNPP at 298 K.

4. CONCLUSION

- The **BNPP** act as a good inhibitorfor the corrosion of C38 steel in 0.5M H_2SO_4solution,the inhibiting effect of **BNPP** increases with increasing inhibitor concentrationand reached a maximum at 10^{-3} M.
- Polarization study showed that the compound under investigation was mixedtype inhibitor.
- Results from weight loss, electrochemical impedance spectroscopy andpolarization curves were in good agreement.
- The efficiency of inhibition by **BNPP** decreased with increasing temperature andits addition led to a increase of the activation energy for corrosion.
- The adsorption is a spontaneous process and obey Langmuir adsorption isotherm. The parameter of adsorption free activation energy (ΔG_{ads}) indicates that the adsorption of inhibitor involve chemisorption.
- BNPP possibly will offer electrons to the metal surface through HOMO (bromine atom, pyridine ring, imidazole and nitro group) and receive electrons from the metal surface through LUMO (imidazole and nitro group).

ACKNOWLEDGMENTS

Prof. Y. KARZAZI extends his appreciation to the Laboratory for Chemistry of Novel Materials, University of Mons, Belgium, for access to the computational facility.

REFERENCES

1. G. Trabanelli,**Corrosion. 47, 410 (1991)**.

2. A. Chetouani, K. Medjahed, K.E. Benabadji, B. Hammouti, S. Kertit, A. Mansri**, Prog. Org. Coat. 46,312 (2003).**

3. B.V. Appa Rao, Md. Yakub Iqbal, B. Sreedhar, **Electrochim. Acta. 55,620 (2010).**

4. G. Avcı, Mater. **Chem. Phys.112, 234 (2008).**

5. A. Döner, R. Solmaz, M. Özcan, G. Kardas, **Corros. Sci. 53,2902 (2011).**

6. A. Popova, M. Christov, S. Raicheva, E. Sokolova,**Corros. Sci. 46,1333 (2004).**
7. I.B. Obot, N.O. Obi-Egbedi, S.A. Umoren, **Corros. Sci. 51,276 (2009).**
8. F. Bentiss, M. Traisnel, L. Gengembre, M. Lagrenée, **Appl. Surf. Sci. 161,194 (2000).**
9. L. Wang, **Corros. Sci. 43,2281 (2001).**
10. L. Wang, **Corros. Sci. 48,608 (2006).**
11. E.A. Noor, **Corros. Sci. 47,33 (2005).**
12. X.H. Li, S.D. Deng, H. Fu, Mater**. Chem. Phys. 115,815 (2009).**
13. X.H. Li, S.D. Deng, H. Fu,.**Corros. Sci. 53,3704 (2011).**
14. L. Malki Alaoui, B. Hammouti, A. Bellaouchou, A. Benbachir, A. Guenbour, S. Kertit.**Der Pharma Chemica. 3,353 (2011).**
15. K. Tebbji, A. Aouniti, A. Attayibat, B. Hammouti, H. Oudda, M. Benkaddour, S. Radi, A.Nahle,.**Indian J. Chem. Technol. 18,244 (2011).**
16. K. Tebbji, H. Oudda, B. Hammouti, M. Benkaddour, S.S. Al-Deyab, A. Aouniti, S. Radi, A. Ramdani,.**Res. Chem. Intermed. 37, 985 (2011).**
17. R. Salghi, L. Bazzi, B. Hammouti, E. Zine, S. Kertit, S. El Issami, E. AitEddi, Bull. **Electrochem. 17, 429 (2001).**
18. M. Elouafi, B. Hammouti, H. Oudda, S. Kertit, R. Touzani, A. Ramdani,. Anti-Corros. **Methods Mater. 49, 15 (2002)15.**
19. S. El Issami, L. Bazzi, A. Benlhachemi, R. Salghi, B. Hammouti, S. Kertit,.**Pigment ResinTech. 36,161 (2007).**
20. F. Bentiss, M. Traisnel, H. Vezin, M. Lagrenee,. **Corros. Sci. 45,371 (2003).**
21. K. Bekkouch, A. Aouniti, B. Hammouti, S. Kertit,. **J. Chim. Phys. 96,838 (1999**).
22. M.A. Quraishi, R. Sardar,.**Corrosion. 58,748 (2002).**
23. D. Ben Hmamou, M. R. Aouad, R. Salghi, A. Zarrouk, M. Assouag, O. Benali, M. Messali, H. Zarrok, B. Hammouti,.**J.Chem. Pharma.Res.4 (7), 3489 (2012).**
24. D. Ben Hmamou, M. R. Aouad , R. Salghi, A. Zarrouk, M. Assouag, O. Benali, M. Messali, H. Zarrok, B. Hammouti,.**J. Chem. Pharma. Res.4 (7), 3498 (2012).**
25. S. Kertit, B. Hammouti,**Appl. Surf. Sci. 93, 59 (1996).**
26. K.F. Khaled, N.S. Abdelshafi, A. El-Maghraby, N. Al-Mobarak, **J. Mater. Environ. Sci. 2, 166 (2011).**
27. S. Kertit, H. Essouffi, B. Hammouti, M. Benkaddour, **J. Chim. Phys. 95, 2072 (1998).**
28. E.-S.M. Sherif, Mater. **Chem. Phys.129,961 (2011).**
29. A. Dafali, B. Hammouti, A. Aouniti, R. Mokhlisse, S. Kertit, K. Elkacemi, **Ann. Chim. Sci. Mater.25,437 (2000).**
30. M. Mousavi, M. Mohammadalizadeh, A. Khosravan, **Corros. Sci. 53,3086 (2011).**
31. A. Dafali, B. Hammouti, S. Kertit, **J. Electrochem. Soc. India. 50,62 (2001).**
32. M. Benabdellah, A. Ousslim, B. Hammouti, A. Elidrissi, A. Aouniti, A. Dafali, K. Bekkouch, M. Benkaddour,.**J. Appl. Electrochem. 37, 819 (2007).**
33. M. Abdallah, H.E. Megahed, M. Sobhi,.**Monatshefte fur Chem. 141,1287 (2010).**

32. M. Bouklah, A. Ouassini, B. Hammouti, A. El Idrissi,. **Appl. Surf. Sci. 250, 50 (2005).**

34. O. Krim, A. Elidrissi, B. Hammouti, A. Ouslim, M. Benkaddour,.**Chem. Eng. Commun. 196,1536 (2009).**

35. K. Bouhrira, F. Ouahiba, D. Zerouali, B. Hammouti, M. Zertoubi, N. Benchat,.**E-J Chem 7(S1),S35 (2010).**

36. A. Chetouani, B. Hammouti, K. Medjahed, A. Mansri,.**Der Pharma Chem. 3, 307 (2011).**

37. R. Saddik, M. Khoutoul, N. Benchat, B. Hammouti, S. El Kadiri, R. Touzani, **Res.ChemlIntermed. 38(9), 2457 (2012).**

38. A. Anejjar, A. Zarrouk, R. Salghi, D. Ben Hmamou, H. Zarrok, S. S. Al-Deyab, M. Bouachrine, B. Hammouti, N. Benchat,**. Int. J. Electrochem. Sci. 8 (4), 5961 (2013).**

39. Ghazoui, R. Saddik, B. Hammouti, A. Zarrouk, N. Benchat, M. Guenbour, S. S. Al-Deyab, I. Warad, **Res. Chem. Intermed. 39 (6),2369 (2013).**

40. A. Anejjar, R. Salghi, A. Zarrouk, O. Benali, H. Zarrok, B. Hammouti, S.S. Al-Deyab, N. Benchat, A. Elaatiaoui, **Int. J. Electrochem. Sci. 8 (9), 11512 (2013).**

41. A. Anejjar, R. Salghi, A. Zarrouk, H. Zarrok, O. Benali, B. Hammouti, S.S. Al-Deyab, N. Benchat, R. Saddik, .**Res. Chem. Intermed.41,913 (2015).**

42. A. Ghazoui, A. Zarrouk, N. Benchat, M. El Hezzat, B. Hammouti, A. Guenbour, R. Salghi,.**Der Pharma. Lett. 5 (4), 247 (2013).**

43. D. Ben Hmamou, R. Salghi, A. Zarrouk, H. Zarrok, B. Hammouti, S.S. Al-Deyab, A. El Assyry, N. Benchat, M. Bouachrine, **Int. J. Electrochem. Sci. 8 (9), 11526 (2013).**

44. L. Afia, N. Rezki, M. R. Aouad, A. Zarrouk, H. Zarrok, R. Salghi, B. Hammouti, M. Messali, S.S. Al. Deyab, **Int. J. Electrochem. Sci. 8 (3), 4346 (2013).**

45. L. Herrag, B. Hammouti, S. Elkadiri, A. Aouniti, C. Jama, H. Vezin, F. Bentiss,.**Corros. Sci. 52, 3042 (2010).**

46. X. Wang, H. Yang, F. Wang,.**Corros. Sci. 53, 113 (2011).**

47. A. D. J. Becke,.**Chem. Phys. 96, 2155 (1992).**

48. A. D. J Becke,.**Chem. Phys.98, 1372 (1993).**

49. C. Lee, W. Yang, R. G. Parr,.**Phys. Rev. B.37, 785 (1988).**

50. M. J. Frisch, G. W. Trucks, H. B. Schlegel, G. E. Scuseria, M. A. Robb, J. R. Cheeseman, G. Scalmani, V. Barone, B. Mennucci, G. A. Petersson, H. Nakatsuji, M. Caricato, X. Li, H. P. Hratchian, A. F. Izmaylov, J. Bloino, G. Zheng, J. L. Sonnenberg, M. Hada, M. Ehara, K. Toyota, R. Fukuda, J. Hasegawa, M. Ishida, T. Nakajima, Y. Honda, O. Kitao, H. Nakai, T. Vreven, J. A. Montgomery, Jr., J. E. Peralta, F. Ogliaro, M. Bearpark, J. J. Heyd, E. Brothers, K. N. Kudin, V. N. Staroverov, T. Keith, R. Kobayashi, J. Normand, K. Raghavachari, A. Rendell, J. C. Burant, S. S. Iyengar, J. Tomasi, M. Cossi, N. Rega, J. M. Millam, M. Klene, J. E. Knox, J. B. Cross, V. Bakken, C. Adamo, J. Jaramillo, R. Gomperts, R. E. Stratmann, O. Yazyev, A. J. Austin, R. Cammi, C. Pomelli, J. W. Ochterski, R. L. Martin, K. Morokuma, V. G. Zakrzewski, G. A. Voth, P. Salvador, J. J. Dannenberg, S. Dapprich, A. D. Daniels, O. Farkas, J. B. Foresman, J. V. Ortiz, J. Cioslowski, and D. J. Fox, **Gaussian, Inc , Wallingford CT, 2010.**

51. B. Donnelly, T.C. Downie, R. Grzeskowiak, H.R. Hamburg, D. Short,.**Corros. Sci. 18, 109 (1978).**

52. H. Zarrok, A. Zarrouk, R. Salghi, M. Assouag, B. Hammouti , H. Oudda, S. Boukhris , S. S. Al Deyab, I. Warad,.**Der Pharmacia Lettre. 5(2),43 (2013).**

53. K.F. Khaled, A. El-Maghraby,.**Arab. J. Chem. 7(3), 319 (2014).**

54. F. Xu, B. Hou, Acta Metall. **Sin. (Engl. Lett.). 22(4), 247 (2009).**

55. O. Benali, H. Benmehdi, O. Hasnaoui, C. Selles, R. Salghi**,. J. Mater. Environ. Sci. 4(1), 127 (2013).**

56. H.B. Ouici, O. Benali, Y. Harek, L. Larabi, B. Hammouti, A. Guendouzi, **Res. Chem.Intermed.39, 2777 (2013).**

57. P. Li, J.Y. Li, K.L. Tan, J.Y. Lee,.**Electrochim. Acta. 42,605 (1997).**

58. N. Labjar, M. Lebrini, F. Bentiss, N.E. Chihib, S. El Hajjaji, C. Jama,. **Mater.Chem. Phys. 119, 330 (2010).**

59. D. Ben Hmamou, R. Salghi, A. Zarrouk, O. Benali, F. Fadel, H. Zarrok, B. Hammouti,.**Int. J. Ind. Chem. 3 (25),1 (2012).**

60. H.J.W. Lenderink, M.V.D. Linden, J.H.W. De Wit**,.Electrochim. Acta. 38, 1989 (1993).**

61. A.K. Singh, M.A. Quraishi,.**Corros. Sci. 52, 152 (2010).**

62. T. Tsuru, S. Haruyama, B. Gijutsu,.**J. Jpn. Soc. Corros. Eng. 27, 573(1978).**

63. E. McCafferty, N. Hackerman, **J. Electrochem. Soc. 119, 146 (1972).**

64.M. Lagrenée, B. Mernari, M. Bouanis, M. Traisnel, F. Bentiss,. **Corros. Sci. 44, 573 (2002).**

65. D. Jayaperumal,.**Mater. Chem. Phys. 119, 478 (2010).**

66. O.L. Riggs, **Corrosion Inhibitors (The National Association of Corrosion Engineers (NACE), Houston, (1973).**

67. F.M. Mahgoub, B.A. Abdel-Nabey, Y.A. El-Samadisy,.**Mater. Chem. Phys.120, 104 (2010).**

68. M.S. Morad, A.M. Kamal El-Dean, **Corros. Sci. 48, 3398 (2006).**

69. R. Solmaz, G. Kardas, B. Yazıcı, M. Erbil,.**Colloids Surf. A Physicochem. Eng.Aspects. 312, 7 (2008).**

70. T. Szauer, A. Brandt,.**Electrochim. Acta. 26, 1257 (1981).**

71. Ivanov, E.S. **Inhibitors for Metal Corrosion in Acid Media. Metallurgy, Moscow (1986).**

72. B. Zerga, A . Attayibat, M. Sfaira, M.Taleb, B. Hammout , M. EbnTouhami, , S. Radi, Z. Rais,**J. Appl. Electrochem. 40, 1575 (2010).**

73. S.S. Abd-El-Rehim, S.A.M. Refaey, F. Taha, M.B. Saleh, R.A. Ahmed,.**J. Appl. Electrochem. 31, 429 (2001).**

74. N.M .Guan, L. Xueming, L . Fei. **Mater. Chem. Phys. 86,59 (2004).**

75. ASTM G1-72, **Metal Corrosion, Erosion andWear, Annual Book of ASTM Standards West Conshohocken, PA: ASTM, (1987).**

76. E. A .Noor, A.H .Al-Moubaraki.**Mater. Chem. Phys.110, 145 (2008).**

77. F. Mansfeld, M.W. Kending, S. Tsai, **Corrosion. 37, 301 (1982).**

78. O. Benali, L. Larabi, B. Tabti , Y. Harek,.**Anti-Corros. Met. Mat. 52, 280 (2005).**

79. I. B. Obot, N. O. Obi-Egbedi, **Corros. Sci, 52, 198 (2010).**

80. O. Benali, L. Larabi, S. M. Mekelleche, Y. Harek. **J. Mater. Sci. 41, 7064 (2006).**

81. J. D. Talati, D. K. Gandhi,.**Corros. Sci. 23, 1315 (1983).**

82. G. K. Gomma, M. H. Wahadan,.**Indian J. Chem. Technol. 2, 107 (1995).**

83. Z. Szklarska-Smialowska, J. Mankowski, **Corros. Sci. 18, 953 (1978).**

84. E. E. Ebenso, M. M. Kabanda, T. Arslan, M. Saracoglu, F. Kandemirli, L. C. Murulana, A. K. Singh, S. K. Shukla, B. Hammouti, K. F. Khaled, M .A. Quraishi, I. B. Obot, N. O. Eddy, **Int. J. Electrochem. Sci. 7, 5643 (2012).**

85. H. Hoptop, W. C. Lineberger, **Phys. Chem. Ref. Data, 14, 731 (1985).**

(2015) ; http://revues.imist.ma/?journal=mjpas&page=index